SUPPLEMENTAL MATERIAL:

Torque Spectroscopy of DNA: Base-Pair Stability, Boundary Effects, Backbending, and Breathing Dynamics

Florian C. Oberstrass[1], Louis E. Fernandes[2], Paul Lebel[3], and Zev Bryant[1,4*]

[1] Department of Bioengineering, Stanford University, Stanford, CA 94305, USA

[2] Program in Biophysics, Stanford University, Stanford, CA 94305, USA

[3] Department of Applied Physics, Stanford University, Stanford, CA, 94305, USA

[4] Department of Structural Biology, Stanford University Medical Center, Stanford, CA 94305, USA

SUPPLEMENTARY METHODS

DNA and magnetic bead preparation. DNA and beads were prepared according the procedures described earlier [1]. DNA molecules were generated by serial ligation of purified restriction digested PCR products (STab. S3 and S4). The component fragments include a segment containing multiply incorporated dUTP-fluorescein (Roche) for torsionally constrained magnetic bead attachment, a segment containing six internal digoxigenin modifications for torsionally constrained coverslip attachment, and a segment containing two internal biotin modifications for rotor bead attachment. Annealing of two 5' phosphorylated oligonucleotides was used to generate SOI inserts (STab. S3). Magnetic beads were MyOne carboxy-modified beads (Dynal) coated with anti-fluorescein (Invitrogen).

Flow cell preparation and tether assembly. As in our previous work [1], flow cells were assembled using Nescofilm gaskets and hole-punched coverslips, with the objective-side cover glass spin-coated with nitrocellulose. Channels were incubated with anti-digoxigenin (Roche, 1.5 μg/ml in PBS, pH 7.4) for 30' and then washed and incubated with blocking buffer (5 mg/ml BSA, PBS, pH 7.4) for 1h. Rotor beads were washed with blocking buffer and incubated with 3 μl DNA (diluted in 10 mM Tris-Cl, pH 8.5, 5 mM EDTA) for 1h. "Power-Bind* Streptavidin Coated Particles" (Thermo Scientific; nominal diameter: 0.3 μm) were used as rotor beads. Flow cells were incubated with preassembled rotor bead-DNA complexes for 1h, washed with blocking buffer, incubated with magnetic beads for 20', and washed again with blocking buffer before exchanging into imaging buffer (10 mM Tris-Cl, pH 7.4, 0.5 mg/ml BSA and 5 mM EDTA).

Data collection and analysis. All measurements were performed at ambient temperature (22 ± 1 ºC) in imaging buffer. DNA tethers were held under 4 pN of tension using magnetic tweezers [1]. Measurements were performed as in [1], except that rotor beads were imaged using objective-side evanescent scattering [2]. Video data were acquired at 250 Hz. During

under- and overwinding, the total twist θ was ramped linearly by rotating the magnets with a constant velocity of 10 deg/s. The torsional spring constant of the transducer κ_{TD} was calibrated by analyzing rotor bead fluctuations of top-only constrained tethers, using the equipartition relationship: $\kappa_{TD} = k_B T / \langle \Delta\psi^2 \rangle$, where the measured angular variance $\langle \Delta\psi^2 \rangle$ = 15.0 ± 0.7 rad^2 (mean ± s.d. based on 8 independent molecules each observed for 400 s). Determination of the magnet angle corresponding to $\theta = 0$ was accomplished using one of three methods: (1) finding the angle that gives maximum extension of the full molecule under low tension [3], (2) recording the angular change of the rotor bead after a molecule becomes unconstrained during data collection, or (3) aligning torque-twist curves by matching the mean torque value during a transition plateau with corresponding plots for the same SOI, calibrated using methods 1 or 2. Methods of zeroing are indicated in Supplementary Table S1. Torque-twist data for individual experiments were binned in intervals of 0.2 rotations for averaging prior to model fitting; average fit parameters are reported in Supplementary Table S1. To idealize time-dependent torque traces under fixed twist conditions, we first smoothed the data over a 1 s window and then used the segmental k-means algorithm [4] with a 2-state model in which the center and widths of the angular distributions for the two states were set based on fitting a double Gaussian distribution to the torque histogram for the trace. For each twist condition, 800 s of data were collected, containing between 40 and 200 transitions.

SUPPLEMENTARY EQUATIONS

2-state transitions in fixed twist and fixed torque ensembles. As a prelude to presenting the Ising-type models used to analyze torque-twist curves for SOIs, we first consider a simple two-state system: A polymer with torsional stiffness κ_0 can transition to an alternative structural state with accompanying changes in equilibrium twist $\Delta\theta_0$, compliance Δc_t and free energy ΔG_0. The partition function $Z(\theta)$ for the fixed twist ensemble is given by the sum of two terms corresponding to the two available states [1]:

$$Z(\theta) = e^{-\beta\frac{1}{2}\kappa_0\theta^2} + \sqrt{\frac{\kappa_1}{\kappa_0}}e^{-\beta\left[\frac{1}{2}\kappa_1(\theta-\Delta\theta_0)^2+\Delta G_0\right]} \quad [S1]$$

where $\kappa_1 = \frac{\kappa_0}{1+\Delta c_t\kappa_0}$. The mean torque for a given imposed twist is given by

$$\langle\tau\rangle(\theta) = -\frac{1}{\beta}\frac{\partial log Z(\theta)}{\partial\theta} = \frac{\kappa_0\theta e^{-\beta\frac{1}{2}\kappa_0\theta^2}+\kappa_1(\theta-\Delta\theta_0)\sqrt{\frac{\kappa_1}{\kappa_0}}e^{-\beta\left[\frac{1}{2}\kappa_1(\theta-\Delta\theta_0)^2+\Delta G_0\right]}}{Z(\theta)} \quad [S2]$$

Torque-twist curves in the fixed twist ensemble can be non-monotonic (SFig. S7), exhibiting "backbending" behavior as discussed for DNA buckling [5], analogous systems such as the Ising model at fixed magnetization [6], and our previous work [1].

The fixed torque partition $Z(\tau)$ may be recovered from the fixed twist partition function using a Laplace transform:

$$Z(\tau) = \int_{-\infty}^{+\infty} Z(\theta)e^{\beta\tau\theta}d\theta \quad [S3]$$

yielding (after dropping a multiplicative constant)

$$Z(\tau) = e^{\beta\frac{\tau^2}{2\kappa_0}} + e^{-\beta\left[\Delta G_0-\frac{\tau^2}{2\kappa_1}-\tau\Delta\theta_0\right]} \quad [S4]$$

The mean twist as a function of imposed torque is then given by

$$\langle\theta\rangle(\tau) = \frac{1}{\beta}\frac{\partial log Z(\tau)}{\partial \tau} = \frac{\frac{\tau}{\kappa_0}e^{\beta\frac{\tau^2}{2\kappa_0}+\left(\frac{\tau}{\kappa_1}+\Delta\theta_0\right)e^{-\beta\left[\Delta G_0-\frac{\tau^2}{2\kappa_1}-\tau\Delta\theta_0\right]}}}{Z(\tau)} \quad [S5]$$

Torque-twist curves in this ensemble are strictly monotonic with positive slope [5] (SFig. S7).

Models for fixed and free boundary conditions. We used an Ising-type model to describe transitions in homogenous SOIs of length *N* basepairs [1]. Each basepair is independently allowed to adopt one of two states with differences in free energy ΔG_0, twist $\Delta\theta_0$ and compliance* Δc_t. In any given configuration, *n* basepairs in the high-energy state are distributed among *d* domains. Cooperativity arises from a free energy penalty *J* at each domain wall between differing states. Under ***fixed boundary conditions*** the penalty *J* is also applied for domain walls at the edge of the SOI adjacent to the handles, which are assumed to remain in B-form. Under these conditions the partition function in the fixed twist ensemble is given by [1]†

$$Z(\theta) = e^{-\beta\frac{1}{2}\kappa_0\theta^2} + \sum_{n=1}^{N}\sum_{d=1}^{\min(n,N-n+1)}\binom{n-1}{d-1}\binom{N-n+1}{d}\sqrt{\frac{\kappa_n}{\kappa_0}}e^{-\beta\left[\frac{1}{2}\kappa_n(\theta-n\Delta\theta_0)^2+n\Delta G_0+2dJ\right]} \quad [S6]$$

where $\kappa_n = \frac{\kappa_0}{1+n\Delta c_t\kappa_0}$

* The difference in compliance between (for example) B-DNA and Z-DNA is given by $\Delta c_t = \frac{1}{\overline{\kappa_Z}} - \frac{1}{\overline{\kappa_B}}$ where $\overline{\kappa_B}$ and $\overline{\kappa_Z}$ are the basepair-normalized torsional rigidities of the two states.

† The initial stiffness κ_0 is expected to be given by $\frac{1}{\kappa_0} = \frac{1}{\kappa_{h1}} + \frac{1}{\kappa_{h2}} + \frac{N}{\overline{\kappa_B}}$ where κ_{h1} and κ_{h2} are the stiffnesses of the handles.

The mean values and distributions of parameters such as τ, n, d, and the number of domain walls s can then be calculated from the partition function:

$$< \tau > (\theta) = -\frac{1}{\beta}\frac{\partial log Z(\theta)}{\partial \theta} \quad [S7]$$

$$= \frac{\kappa_0 \theta e^{-\beta\frac{1}{2}\kappa_0\theta^2} + \sum_{n=1}^{N}\sum_{d=1}^{\min(n,N-n+1)}\binom{n-1}{d-1}\binom{N-n+1}{d}\kappa_n(\theta - n\Delta\theta_0)\sqrt{\frac{\kappa_n}{\kappa_0}}e^{-\beta\left[\frac{1}{2}\kappa_n(\theta-n\Delta\theta_0)^2+n\Delta G_0+2dJ\right]}}{Z(\theta)}$$

$$< n > (\theta) = -\frac{1}{\beta}\frac{\partial log Z(\theta)}{\partial \Delta G_0} = \frac{\sum_{n=1}^{N}\sum_{d=1}^{\min(n,N-n+1)}\binom{n-1}{d-1}\binom{N-n+1}{d} n\sqrt{\frac{\kappa_n}{\kappa_0}}e^{-\beta\left[\frac{1}{2}\kappa_n(\theta-n\Delta\theta_0)^2+n\Delta G_0+2dJ\right]}}{Z(\theta)} \quad [S8]$$

$$P(n|\theta) = \frac{\sum_{d=1}^{\min(n,N-n+1)}\binom{n-1}{d-1}\binom{N-n+1}{d}\sqrt{\frac{\kappa_n}{\kappa_0}}e^{-\beta\left[\frac{1}{2}\kappa_n(\theta-n\Delta\theta_0)^2+n\Delta G_0+2dJ\right]}}{Z(\theta)} \quad [S9]$$

$$< s > (\theta) = -\frac{1}{\beta}\frac{\partial log Z(\theta)}{\partial J} = \frac{\sum_{n=1}^{N}\sum_{d=1}^{\min(n,N-n+1)}\binom{n-1}{d-1}\binom{N-n+1}{d} 2d\sqrt{\frac{\kappa_n}{\kappa_0}}e^{-\beta\left[\frac{1}{2}\kappa_n(\theta-n\Delta\theta_0)^2+n\Delta G_0+2dJ\right]}}{Z(\theta)} \quad [S10]$$

$$< d > (\theta) = \frac{\sum_{n=1}^{N}\sum_{d=1}^{\min(n,N-n+1)}\binom{n-1}{d-1}\binom{N-n+1}{d} d\sqrt{\frac{\kappa_n}{\kappa_0}}e^{-\beta\left[\frac{1}{2}\kappa_n(\theta-n\Delta\theta_0)^2+n\Delta G_0+2dJ\right]}}{Z(\theta)} \quad [S11]$$

Under ***free boundary conditions*** (no domain wall penalties assessed at SOI edges) the partition function is given by [1]:

$$Z(\theta) = e^{-\beta\frac{1}{2}\kappa_0\theta^2} \quad \text{[S12]}$$
$$+ 2\sum_{n=1}^{N-1}\sum_{d=1}^{\min(n,N-n)}\binom{n-1}{d-1}\binom{N-n-1}{d-1}\sqrt{\frac{\kappa_n}{\kappa_0}}\,e^{-\beta\left[\frac{1}{2}\kappa_n(\theta-n\Delta\theta_0)^2+n\Delta G_0+(2d-1)J\right]}$$
$$+ \sum_{n=2}^{N-1}\sum_{d=2}^{\min(n,N-n+1)}\binom{n-1}{d-1}\binom{N-n-1}{d-2}\sqrt{\frac{\kappa_n}{\kappa_0}}\,e^{-\beta\left[\frac{1}{2}\kappa_n(\theta-n\Delta\theta_0)^2+n\Delta G_0+2(d-1)J\right]}$$
$$+ \sum_{n=1}^{N-2}\sum_{d=1}^{\min(n,N-n-1)}\binom{n-1}{d-1}\binom{N-n-1}{d}\sqrt{\frac{\kappa_n}{\kappa_0}}\,e^{-\beta\left[\frac{1}{2}\kappa_n(\theta-n\Delta\theta_0)^2+n\Delta G_0+2dJ\right]}$$
$$+ \sqrt{\frac{\kappa_N}{\kappa_0}}\,e^{-\beta\left[\frac{1}{2}\kappa_N(\theta-N\Delta\theta_0)^2+N\Delta G_0\right]}$$

Generalized model: Intermediate cases in which a distinct penalty *J'* is assessed for domain walls at SOI edges can be covered by a generalized model, which encompasses free boundary conditions and fixed boundary conditions as limiting cases with $J' = 0$ and $J' = J$, respectively.

$$Z(\theta) = e^{-\beta\frac{1}{2}\kappa_0\theta^2} \quad \text{[S13]}$$
$$+ 2\sum_{n=1}^{N-1}\sum_{d=1}^{\min(n,N-n)}\binom{n-1}{d-1}\binom{N-n-1}{d-1}\sqrt{\frac{\kappa_n}{\kappa_0}}\,e^{-\beta\left[\frac{1}{2}\kappa_n(\theta-n\Delta\theta_0)^2+n\Delta G_0+(2d-1)J+J'\right]}$$
$$+ \sum_{n=2}^{N-1}\sum_{d=2}^{\min(n,N-n+1)}\binom{n-1}{d-1}\binom{N-n-1}{d-2}\sqrt{\frac{\kappa_n}{\kappa_0}}\,e^{-\beta\left[\frac{1}{2}\kappa_n(\theta-n\Delta\theta_0)^2+n\Delta G_0+2(d-1)J+2J'\right]}$$
$$+ \sum_{n=1}^{N-2}\sum_{d=1}^{\min(n,N-n-1)}\binom{n-1}{d-1}\binom{N-n-1}{d}\sqrt{\frac{\kappa_n}{\kappa_0}}\,e^{-\beta\left[\frac{1}{2}\kappa_n(\theta-n\Delta\theta_0)^2+n\Delta G_0+2dJ\right]}$$
$$+ \sqrt{\frac{\kappa_N}{\kappa_0}}\,e^{-\beta\left[\frac{1}{2}\kappa_N(\theta-N\Delta\theta_0)^2+N\Delta G_0+2J'\right]}$$

A ***one-sided model*** was applied for constructs in which spacers are only incorporated at one of the SOI edges:

$$Z(\theta) = e^{-\beta\frac{1}{2}\kappa_0\theta^2} \qquad \text{[S14]}$$

$$+ \sum_{n=1}^{N-1}\sum_{d=1}^{\min(n,N-n+1)}\binom{n-1}{d-1}\binom{N-n}{d-1}\sqrt{\frac{\kappa_n}{\kappa_0}}e^{-\beta\left[\frac{1}{2}\kappa_n(\theta-n\Delta\theta_0)^2+n\Delta G_0+(2d-1)J+J'\right]}$$

$$+ \sum_{n=1}^{N-1}\sum_{d=1}^{\min(n,N-n)}\binom{n-1}{d-1}\binom{N-n}{d}\sqrt{\frac{\kappa_n}{\kappa_0}}e^{-\beta\left[\frac{1}{2}\kappa_n(\theta-n\Delta\theta_0)^2+n\Delta G_0+2dJ\right]}$$

$$+ \sqrt{\frac{\kappa_N}{\kappa_0}}e^{-\beta\left[\frac{1}{2}\kappa_N(\theta-N\Delta\theta_0)^2+N\Delta G_0+J+J'\right]}$$

SUPPLEMENTARY REFERENCES

[1] F. C. Oberstrass, L. E. Fernandes, and Z. Bryant, Proc Natl Acad Sci U S A **109** (2012).
[2] I. Braslavsky *et al.*, Appl Optics **40** (2001).
[3] T. R. Strick *et al.*, Science **271** (1996).
[4] F. Qin, Biophys J **86** (2004).
[5] J. F. Marko, and S. Neukirch, Phys Rev E Stat Nonlin Soft Matter Phys **85** (2012).
[6] F. Gulminelli *et al.*, Phys Rev E Stat Nonlin Soft Matter Phys **68** (2003).
[7] J. C. Wang, Proc Natl Acad Sci U S A **76** (1979).
[8] M. Y. Sheinin *et al.*, Phys Rev Lett **107** (2011).
[9] Z. Bryant *et al.*, Nature **424** (2003).
[10] I. Ashikawa, K. Kinosita, Jr., and A. Ikegami, Biochim Biophys Acta **782** (1984).
[11] W. R. Bauer, and C. J. Benham, J Mol Biol **234** (1993).
[12] J. F. Marko, Phys Rev E Stat Nonlin Soft Matter Phys **76** (2007).

SUPPLEMENTARY FIGURES & TABLES

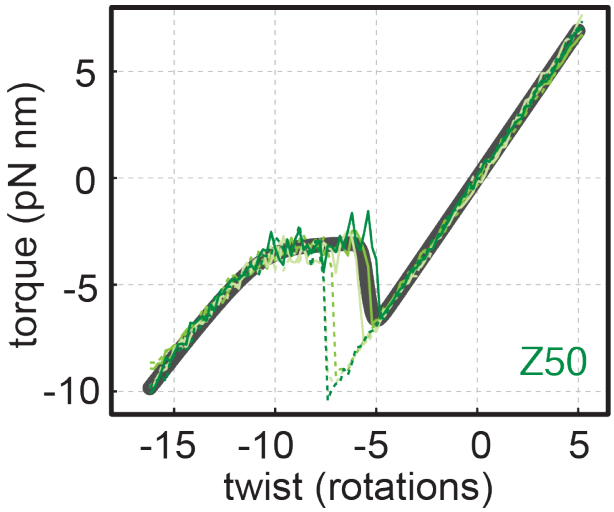

FIG. S1. Fixed boundary conditions: Torque response of Z50. Three independently measured torque-twist plots for 50 bp long d(pGpC)-repeat SOIs (Z50) (green) are shown overlaid with the curve predicted by the model (gray). Dashed lines indicate data collected during unwinding, and solid lines indicate data collected during rewinding. The model shown here uses fixed boundary conditions and is plotted based on averaged parameters from fits to the rewinding curves shown.

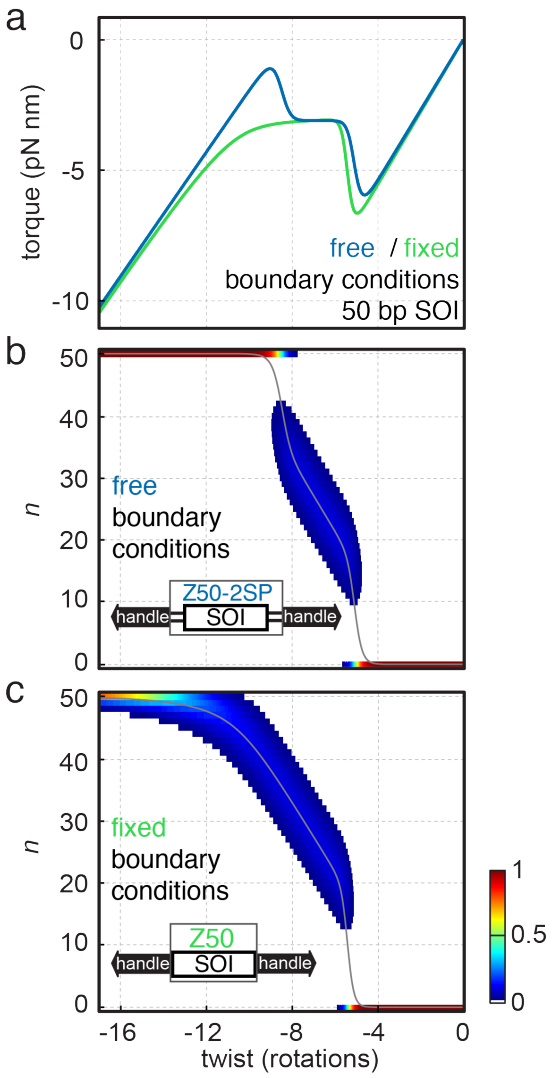

FIG. S2. Calculated behavior of structural transitions in the fixed twist ensemble. (a) Simulated torque-twist plot for a 50 bp long GC-repeat under free (blue) and fixed (green) boundary conditions with parameters measured for Z50 and Z50-2SP, respectively (STab. S1). **(b)** Mean number of nucleotides <*n*> in the high energy state (gray line) and probability distribution *P(n)* (heat map) as a function of imposed twist for the calculation with free boundary conditions shown in (a). **(c)** As in (b), for fixed boundary conditions.

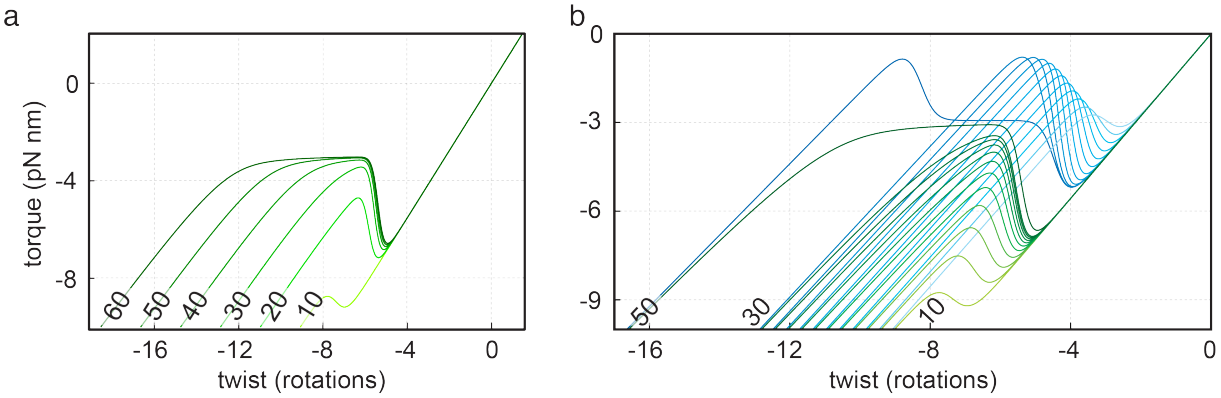

FIG. S3. The effect of SOI length on transitions in under fixed boundary conditions. (a) Series of calculated torque-twist plots using the model with fixed boundary conditions and SOI lengths ranging from N=10 to N=60 basepairs. **(b)** Distinct length-dependent behavior of fixed and free boundary conditions in the low-N regime, which shows approximately two-state behavior. Calculations for N = 30 to N=10 in increments of 2 are shown for free (blue) and fixed boundary conditions (green), alongside reference calculations for N = 50. For all curves, N was varied while all other parameters were kept constant (STab. S1, Z50).

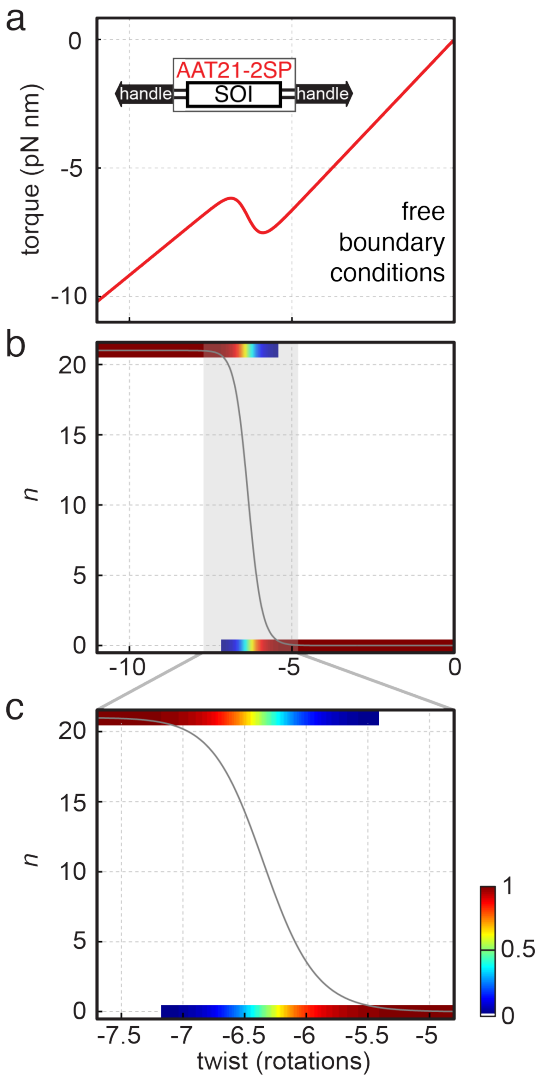

FIG. S4. Short inserts with free boundary conditions are expected to closely approximate two-state behavior. (a) Calculated torque-twist plot for a 21 bp long AAT-repeat with free boundary conditions, using parameters measured for AAT21-2SP (STab. S1). **(b)** Corresponding plots of mean number of nucleotides <*n*> in the high energy state (gray line) and probability distribution *P(n)* (heat map) as a function of twist for AAT21-2SP. **(c)** expanded view of the transition shown in (b).

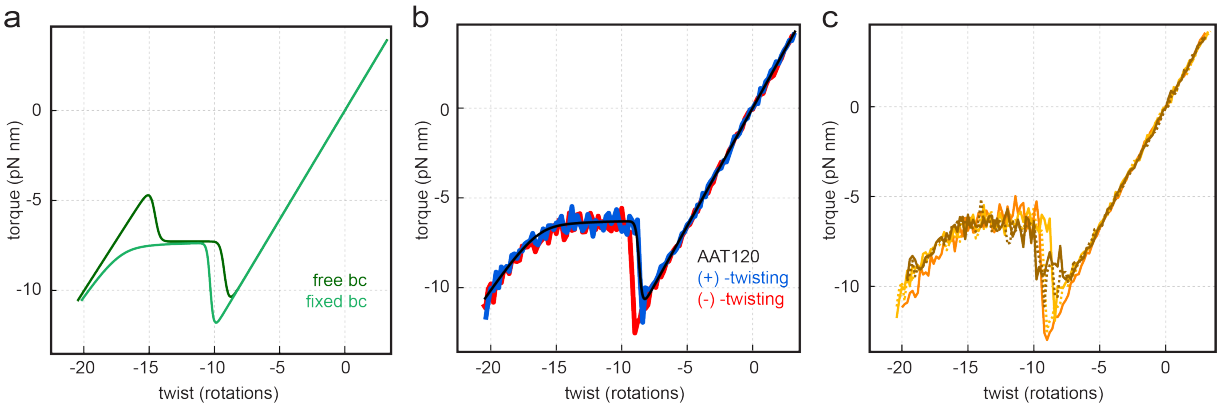

FIG. S5. Response of AAT120 under fixed boundary conditions. (a) Calculated torque-twist plots for 120 basepair AAT-repeats under free (dark green, generalized model) and fixed (light green) boundary conditions using parameters measured for AAT120-2SP (ΔG_0 = 0.62 kcal/mol, J = 7.2 kcal/mol, J' = 0.5 kcal/mol, $\Delta\theta_0$ = -0.58 rad/bp, Δc_t = 0.003 rad/(pN nm bp)) and $1/\kappa_0$ = 5.17 rad/(pN nm), STab. S1). **(b)** Unwinding (red) and rewinding (blue) data are shown for an AAT120 molecule. Using fixed boundary conditions, the best fit (black) to the rewinding curve gives parameters similar to AAT120-2SP measurements: ΔG_0 = 0.54 kcal/mol, J = 6.7 kcal/mol, $\Delta\theta_0$ = -0.58 rad/bp, Δc_t = 0.008 rad/(pN nm bp) and $1/\kappa_0$ = 4.78 rad/(pN nm). **(c)** Unwinding (dashed lines) and rewinding curves (solid lines) for two additional molecules (shown in two different colors) display some heterogeneity, but retain the expected torque signature of fixed boundary conditions as observed in (a). Note**:** peak negative torques in excess of -10 pN nm may be inaccurate because of instability in the transducer DNA segment; the linear assumption used for converting transducer angular displacement to torque is not justified in this regime.

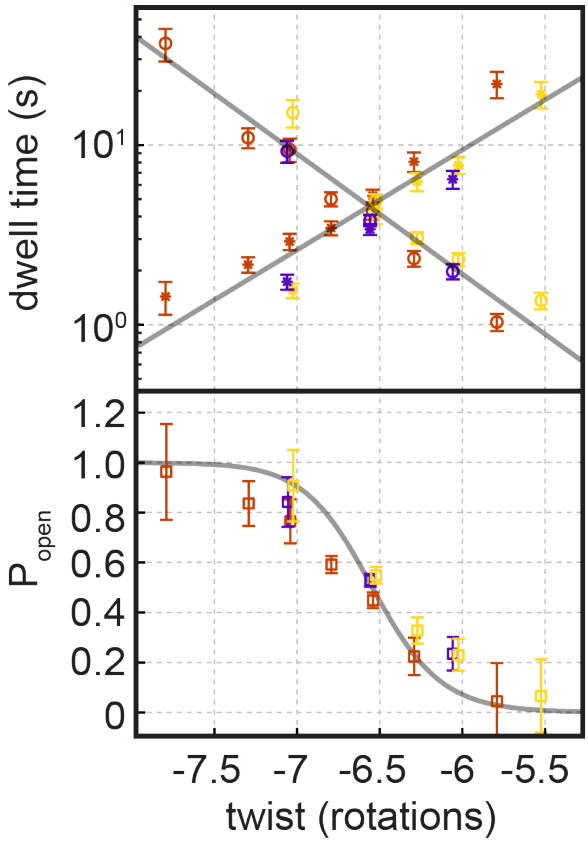

FIG. S6. 'Breathing' dynamics of AAT21-2SP for several DNA tethers. Semi-log plot of mean dwell times <*t*> as a function of total twist imposed on 3 independent DNA tethers are shown (top panel). All probabilities of being in the open state at fixed twists combined are fit using the 2-state model (gray line in bottom panel, Equation S1). The fit gives a total ΔG_0 of ~12 kcal/mol. κ_0, $\Delta\theta_0$ and Δc_t were held constant during fitting (STab. S1, AAT21-2SP). Data in both panels are shown as mean ± s.e.m.

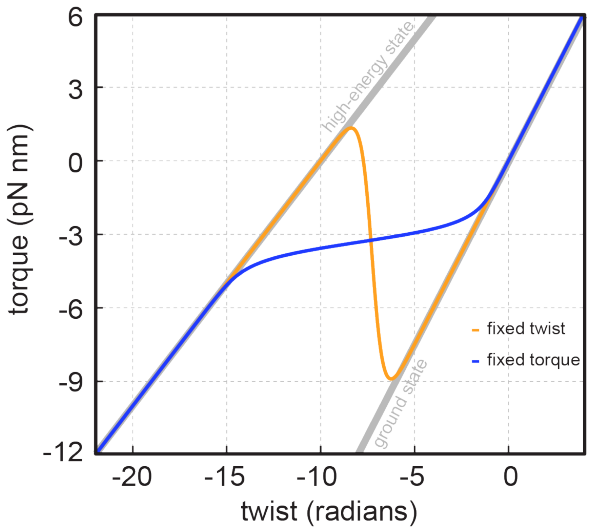

FIG. S7. Comparison of two-state transitions in different ensembles. Under fixed twist conditions the calculated torque-twist plot for two-state system can show backbending (orange line, Equation S2 using κ_0 = 1.5 pNnm/rad, Δc_t = 0.5 pNnm/rad, $\Delta\theta_0$ = -10 rad, and ΔG_0 = 5 kcal/mol), whereas the same system under fixed torque conditions (Equation S5, blue line) shows monotonic behavior.

SOI	N	ΔG_0 (kcal/(mol bp))	J (kcal/mol)	J' (kcal/mol)	$\Delta\theta_0$ (rad/bp)	$1 / \kappa_0$ (rad/pN nm)	Δc_t (rad/(pN nm bp))	# of traces	zeroing
Z50 (fixed)	**50**	0.45 ± 0.05	5.0 ± 0.7	NA	-1.05 ± 0.09	4.52 ± 0.14	0.014 ± 0.012	3+	2E 1A
Z50 (generalized)	**50**	0.45 ± 0.04	5.0 ± 0.7	4.9 ± 0.2	-1.04 ± 0.08	4.52 ± 0.14	0.015 ± 0.012	3+	2E 1A
Z50 (dynamic)[1]	**50**	0.42 ± 0.08	5.0 ± 0.6	NA	-0.79 ± 0.24	3.93 ± 0.22	0.042 ± 0.029	2- 2+	NA
Z50-1SP	**50**	0.50 ± 0.02	6.3 ± 1.1	1.0 ± 0.2	-1.12 ± 0.01	4.53 ± 0.01	0.003 ± 0.003	3+	1E 1U 1A
Z50-2SP	**50**	0.48 ± 0.04	5.6 ± 0.4	0.7 ± 0.5	-1.05 ± 0.02	4.65 ± 0.11	0.013 ± 0.003	3+	2E 1A
AAT120-2SP	**120**	0.62 ± 0.02	7.2 ± 1.1	0.5 ± 0.6	-0.58 ± 0.03	5.17 ± 0.12	0.003 ± 0.003	3- 3+	2E 1A
AAT50-2SP	**50**	0.62*	7.2*	0.5*	-0.51 ± 0.05	4.67 ± 0.09	0.020 ± 0.011	3- 3+	3E
AAT21-2SP	**21**	0.49 ± 0.08	7.2*	0.5*	-0.33 ± 0.20	4.71 ± 0.09	0.065 ± 0.038	3- 3+	3E

TAB. S1. Parameters for structural transitions. Torque-twist curves were fit using the Ising-type models presented in Supplemental Equations. Experimental data were binned in intervals of 0.2 rotations prior to fitting. For fits to Z50, Z50-2SP, Z50-1SP, and AA120-2SP data, N was held fixed and all remaining parameters were optimized using least squares fitting. For AAT50-2SP and AAT21-2SP, $\Delta\theta_0$, Δc_t, and κ_0 were instead obtained from two linear fits to the pre-transition and post-transition regions of the curve; J and J' for these constructs were fixed based on AAT120-2SP. Z50 (generalized) uses the same data as for Z50 (fixed) but was fit using the generalized model, yielding J' indistinguishable from J as expected. Z50 (dynamic) reports values from our previous study using dynamic RBT [1]. Reported parameters are shown as mean ± s.d. of best fit values obtained. Parameters for

Z50, Z50-1SP and Z50-2SP are based on 3 independent (+) rotation experiments (notated “3+”). Parameters for AAT120-2SP, AAT50-2SP and AAT21-SP are based on averages of one (+) winding experiment and one (-) winding experiment for each of three different molecules (notated “3- 3+”). Methods used for twist zeroing were: Maximum extension under supercoiling and low force (E), DNA tether becoming unconstrained after the measurement (U), and alignment to other traces using the torque plateau (A). Number of molecules and method for zeroing are shown. *values based on AAT120-2SP and used for model plotting.

	helicity $\Delta\theta_0$ (rad/bp)	twist persistence length P_t (bp)	free energy change ΔG_0 (kcal/(mol bp))	domain wall penalty J (kcal/mol)
B-DNA	0.60[A]	278[B]	NA	NA
Z-DNA $(GC)_n$	-0.45	18	0.48	5.6
strand-separated $(AAT)_n$	0.02	>35[C]	0.62	7.2

TAB. S2. Summary of parameters describing structural states. These effective parameters correspond to the solution conditions (10 mM Tris-Cl, pH 7.4, 0.5 mg/ml BSA and 5 mM EDTA) and tension (4 pN) used in this study. Values for Z-DNA are based on Z50-2SP (STab. S1). Values for strand-separated DNA are based on AAT120-2SP (STab. S1). [A] B-DNA helicity is based on reference [7]. [B] Effective twist persistence length for B-DNA is calculated from the torsional stiffness of the transducer segment (Supplementary Methods). [C] The measured Δc_t for conversion of B-DNA to strand-separated DNA was approximately equal to the estimated measurement error (STab. S1). A lower bound on the twist persistence length was estimated by calculating the persistence length that would yield a Δc_t equal to twice the measurement error (STab. S1).

Note on persistence lengths: Mixed DNA sequences under negative torques transition to a so-called L-DNA state with left-handed helicity and P_t =20-30 bp [1, 8]. L-DNA may be an aggregate state with significant Z-DNA and strand-separated components [1, 9]. Z50-2SP measurements provide a more confident determination of GC50 Z-DNA stiffness than our previous

work [1] because of the extensive post-transition linear region seen under free boundary conditions (Fig. 2). We measure an effective twist persistence length $P_{t,}$ = 18 ± 4 bp for GC50 in the Z-DNA state, substantially softer than B-DNA and similar to L-DNA. Fluorescence anisotropy measurements [10] have also reported that Z-DNA is torsionally much softer than B-DNA. AAT120-2SP measurements do not show a measureable compliance change associated with strand separation. We and others have suggested a persistence length of 2-7 bp, shorter than L-DNA, for strand-separated DNA [1, 11, 12]. A persistence length in this range would lead to an easily measurable change in compliance for AAT120-2SP; further sequences should be investigated to determine whether this result is general.

Ligation strategy for DNA tethers

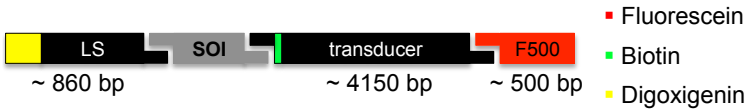

Oligonucleotides for SOIs

Z50	5' ACTGCCGCTGTACACTCAAGGAAAAGCGCGCGCGCGCGCGCGCGCGCGCGCGCGCGCGCGCGCGCGCGCGCGCGCGCGCGCGCGCGCAACTTTGGACAACACTCGGCA 3' GGCGACATGTGAGTTCCTTTTCGCGCGCGCGCGCGCGCGCGCGCGCGCGCGCGCGCGCGCGCGCGCGCGCGCGCGCGCGCGCGCGTTGAAACCTGTTGTGAGCCGTACTG
Z50-SP1	5' ACTGCCGCTGTACACTCAAGGAAAAGCGCGCGCGCGCGCGCGCGCGCGCGCGCGCGCGCGCGCGCGCGCGCGCGCGCGCGCGC-spacer-AACTTTGGACAACACTCGGCA 3' GGCGACATGTGAGTTCCTTTTCGCGCGCGCGCGCGCGCGCGCGCGCGCGCGCGCGCGCGCGCGCGCGCGCGCGCGCGCGCGCG-spacer-TTGAAACCTGTTGTGAGCCGTACTG
Z50-SP2	5' ACTGCCGCTGTACACTCAAGGAAAA-spacer-GCGCGCGCGCGCGCGCGCGCGCGCGCGCGCGCGCGCGCGCGCGCGCGCGCGCGCGCGC-spacer-AACTTTGGACAACACTCGGCA 3' GGCGACATGTGAGTTCCTTTT-spacer-CGCGCGCGCGCGCGCGCGCGCGCGCGCGCGCGCGCGCGCGCGCGCGCGCGCGCGCG-spacer-TTGAAACCTGTTGTGAGCCGTACTG
AAT21-SP2	5' ACTGCCCGAGTGCCCAGG-spacer-ATTATTATTATTATTATTATT-spacer-GCGCTGAGTGTGGGCCCACAGGGG 3' GGGCTCACGGGTCC-spacer-TAATAATAATAATAATAATAA-spacer-CGCGACTCACACCCGGGTGTCCCCACTG
AAT50-SP2	5' ACTGCCCGAGTGCCCAGG-spacer-AATAATAATAATAATAATAATAATAATAATAATAATAATAATAATAA-spacer-GCGCTGAGTGTGGGCCCACAGGGG 3' GGGCTCACGGGTCC-spacer-TTATTATTATTATTATTATTATTATTATTATTATTATTATTATTATT-spacer-CGCGACTCACACCCGGGTGTCCCCACTG
AAT120	5' ACTGCCCGAGTGCCCAGG-$(AAT)_{40}$-GCGCTGAGTGTGGGCCCACAGGGG 3' GGGCTCACGGGTCC-$(TTA)_{40}$-CGCGACTCACACCCGGGTGTCCCCACTG
AAT120-SP2	5' ACTGCCCGAGTGCCCAGG-spacer-$(AAT)_{40}$-spacer-GCGCTGAGTGTGGGCCCACAGGGG 3' GGGCTCACGGGTCC-spacer-$(TTA)_{40}$-spacer-CGCGACTCACACCCGGGTGTCCCCACTG
spacer	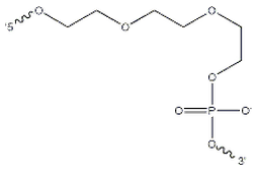

TAB. S3. Schematics for DNA tether ligation and sequences of interest (SOIs). Building blocks for DNA tethers were generated by PCR (STab. S4), except for the SOI segment. F500 was PCR amplified using modified dNTPs for incorporation of fluorescein labels. PCRs for the lower segment (LS) and the transducer region were performed using primers with biotin or digoxigenin

modifications, shown as green and yellow boxes. SOIs consist of two 5' phosphorylated oligonucleotides (Integrated DNA Technologies, Inc.), which were mixed in equimolar ratio in PBS, heated to 94 °C for 5 min, and annealed by gradually cooling to 4°C. For atomic spacers we used triethylene glycol spacer 9, which can be integrated during commercial synthesis of oligonucleotides.

PCRs for single molecule tethers				
	Primer	**Length**	**Template**	**Digest**
F500	GATCGAAGACACTTAGACAACCCACAAGTATAGAGGCTCCTATG GACGCGGATATAATGACATTTCCTAAC	520	pFO-SE1	BbsI
transducer	GAAGGGTCTCATGACTCACTATAGGGCGAATTGGAGCTCCACCGCG GAAGGGTCTCACTAACACTAAAGGGAACAAAAGCTGGGTAC	4156	pFO-SE2	BsaI
LS	GGAAGGAGATTCTCGACAGTTCTAATTGACCTCTTACCTTTTCCCAGTTCAATCTTTGTCAAACACC GTAGGAAGACACCAGTGGAGTCTCCAGAACCTTAAAGAAG	879	pFO-2S	BbsI

TAB. S4. Building blocks for preparative ligation of DNA tethers. Primers, templates (described in [1]) and resulting lengths of the PCR products (in bp) are displayed. PCR products were digested with the enzymes indicated. Modifications are highlighted: Yellow indicates 5' digoxigenin and internal digoxigenin-dT. Green indicates an internal biotin-dT modification. Primers were synthesized by Integrated DNA Technologies, Inc. or Alpha DNA.